Journal of Supramolecular Structure 10:79–96
Normal and Abnormal Red Cell Membranes 343–360

Membrane Protein Organization in ATP-Depleted and Irreversibly Sickled Red Cells

J. Palek and S.C. Liu

Department of Research, St Elizabeth's Hospital of Boston, and Tufts University School of Medicine, Boston, Massachusetts

It has been proposed that the spectrin-actin submembrane network participates in control of red cell shape and deformability. We have examined ATP- and calcium-dependent changes in organization of spectrin in the membrane employing cross-linking of the nearest membrane protein neighbors by spontaneous or catalyzed ($CuSO_4$, O-phenanthroline) intermolecular disulfide couplings and two-dimensional sodium dodecyl sulfate polyacrylamide gel electrophoresis.

Cross-linking of fresh red cells resulted in the formation of spectrin and actin dimers and tetramers. ATP-depleted red cells differed from fresh cells in the presence of an additional reducible polymer of $MW > 1 \times 10^6$ selectively enriched in spectrin. This polymer formed spontaneously when red cells were depleted of ATP under aerobic conditions. After anaerobic ATP depletion, the polymer formed in ghosts after cross-linking by catalytic oxidation. Polymerization was prevented by maintenance of ATP and coincided with an ATP-dependent discocyte-echinocyte transformation. This suggests that, in ATP-depleted red cells, spectrin is rearranged to establish closer contacts, and that this may contribute to the discocyte-echinocyte transformation.

The introduction of greater than 0.5 mM Ca^{++} into ghosts by inclusion in hemolysis buffer or into fresh red cells (but not ATP-depleted red cells) by treatment with ionophore A23187 spontaneously produced a nonreducible polymer which others have attributed to transamidative cross-linking of spectrin, band 3, and other proteins. Spontaneous formation of both polymer types (reducible in aerobically ATP-depleted red cells and nonreducible in fresh, Ca^{++} enriched red cells) resulted in stabilization ("autocatalytic fixation") of spheroechinocytic shape.

Irreversibly sickled cells, which have increased calcium and decreased ATP, and exhibit a permanent membrane deformation, failed to form any of the above polymers. This suggests that in contrast to normal cells depleted of ATP

Abbreviations: ATP – adenosine triphosphate, ISCs – irreversibly sickled cells, HEPES – N_2 hydroxyethyl piperazine N'2-ethane sulphonic acid, SDS – sodium dodecylsulphate, PAGE – polyacrylamide gel electrophoresis, DTT – dithiothreitol, SEM – scanning electron microscopy, G6PD – glucose 6-phosphate dehydrogenase, EDTA – ethylenediaminotetracetic acid, A23187 – calcimycin, HbSS – sickle cell anemia.

Received May 4, 1978; accepted September, 11, 1978.

0091-7419/79/1001-0079$03.20

in vitro, fixation of ISC shape in vivo is not related to Ca- and ATP-dependent membrane protein polymerization. However, ISCs had an increased propensity to form the reducible, spectrin-rich polymer during a subsequent metabolic depletion in vitro. This was associated with transformation of ISCs into spheroechinocytes. Similar echinocytic ISCs were found to constitute 5–10% of the densest fractions of freshly separated ISCs. ISCs then exhibit spheroechniocyte transformation, both in vitro and in vivo. We propose that this is due to spectrin reorganization that presumably results from the progressively increasing calcium and decreasing ATP of ISCs.

These data provide evidence of altered spectrin organization in membranes of ATP-depleted, calcium-enriched red cells in vitro and in vivo.

Key words: red cell membrane proteins, spectrin, red cell shape, deformability, membrane protein cross-linking, membrane protein disulfide coupling, red cell adenosine triphosphate, calcium, membrane protein polymerization, discocyte–echinocyte transformation, irreversibly sickled cells, sickle cell anemia

Viscoelastic properties of erythrocyte membranes are principally determined by the two-dimensional network of peripheral membrane proteins spectrin and actin, laminating the internal side of the membrane [1–4]. Changes in physical properties and molecular organization of these proteins in red cells undergoing decrease in intracellular ATP and accumulation of calcium have been implicated in alterations of cell shape, deformability, and membrane stability [5–8].

In this review, we examine the organization of spectrin and other membrane proteins in red cell membranes as a function of intracellular ATP and calcium concentrations in vitro, and we discuss their possible significance for the control of cell shape and deformability. We further report our studies on membrane protein organization of irreversibly sickled cells, which exhibit increased calcium [9–10], and a decreased ATP content [11, 12]. Their stabilization in an irreversibly sickled shape has been related to a permanent deformation of their membranes [13]. We employed cross-linking of nearest membrane protein neighbors by intermolecular disulfide couplings produced by catalytic oxidation of red cell ghosts or by spontaneous oxidation during aerobic incubation of intact red cells.

MATERIALS AND METHODS

Venous blood was collected into heparin Vacutainers, red cells were separated by centrifugation and washed, and white cells and platelets were removed by aspiration of the buffy coat after each washing. Red cells were suspended at 20% hematocrit in an isotonic solution containing 50 mM glycylglycine (pH 7.4 at 37°C), 5 mM KCl, 2 mM $CaCl_2$, 2 mM $MgCl_2$, and NaCl to 290 mOsm and were incubated under air or nitrogen with gentle mixing [14]. At specified times, red cells were separated from supernatants and white ghosts were prepared by hemolysis in 30 volumes of 10 mM Tris-HCl buffer (pH 7.4) followed by two washings [14]. Part of the ghost pellet was subjected to oxidative cross-linking by reacting the ghosts with 30 volumes of $CuSO_4$ (10 μM), O-phenanthroline (50 μM), at 25°C for 10 min. Selected samples were also cross-linked with 2 mM glutaraldehyde in 10 mM HEPES (pH 7.4) at 25°C for 30 min. The details have been described previously [15, 16].

Ghosts were solubilized in SDS solution and subjected to two-dimensional PAGE [17]. In analyzing cleavable (oxidative) cross-linkings, membrane proteins were first separated in cylindrical gels without DTT reduction. The composition of the cross-linked complexes was identified by placing the first-dimension gels horizontally on the top of the

second-dimension slab gel. After passage through a DTT zone to cleave the intermolecular disulfide crosslinks, membrane proteins were separated in the second dimension on the slab gels and identified according to their relative mobilities as compared to a standard membrane sample. In some examples, the proteins of the cross-linked complexes were quantified by densitometric scanning of Coomassie blue-stained gels [14].

Venous blood of patients with the homozygous form of sickle cell anemia was fractionated on discontinuous stractan gradients [18] to yield ISC-rich fractions. ISCs were identified according to criteria described by Bertles and Milner [19] by phase contrast microscopy and SEM [20]. ATP and GSH were measured as detailed by Beutler [21].

RESULTS

Oxidation-Induced Membrane Protein Cross-linkings

The two-dimensional electrophoresis of membrane proteins from fresh red cells not exposed to cross-linking is illustrated in Figure 1A. The stained replica of the first-dimension cylindrical gel is positioned horizontally on top of the slab gel. After electrophoresis in the second dimension, membrane proteins separated, forming a skewed line. The individual spots were identified from their relative mobilities as compared to a reference membrane sample in an identical gel system and denoted by arabic numerals according to Fairbanks et al [22]. The dotted circles represent glycoproteins [14]. No off-diagonal spots are noted in the second dimension, indicating the absence of spontaneous oxidative cross-links in fresh red cell membranes immediately subjected to SDS PAGE.

Two-dimensional separation of membrane proteins from fresh ghosts subjected to mild catalytic oxidation (20 mM $CuSO_4$, 50 mM O-phenanthroline, 25°C, 10 min) is illustrated in Figure 1B. On the replica of the first-dimension gel, a band corresponding to MW 450,000 can be seen (first vertical arrow). After DTT cleavage and subsequent separation in the second dimension, this band can be identified as the spectrin 1 + 2 heterodimer, as indicated by the presence of these polypeptides as off-diagonal spots positioned in the same vertical line as the original complex. Additional complexes include spectrin tetramers; complexes of spectrin polypeptide 2 and band 4.9; dimers, trimers, and tetramers of band 3; and dimers of band 4.1, 4.5, and 5.

The two-dimensional separation of ATP-depleted red cell membrane proteins cross-linked by catalytic oxidation is illustrated in Figure 1C. ATP depletion was achieved by 22 h incubation (37°C) in a buffered solution without glucose. Anaerobic conditions were used to avoid spontaneous membrane protein oxidation. The cross-linking pattern of membrane proteins from ATP-depleted cells differed from that of fresh red cells in that a polymer of very high mw ($> 1 \times 10^6$) was present at the origin of the first dimension gel (note asterisk, Fig 1C). This complex was completely dissociated by DTT reduction and separated into multiple components, which include spectrin polypeptides 1 and 2; polypeptides 3, 4.5, 5; and other less easily identified components. A similar complex was formed spontaneously when red cells were incubated to deplete their ATP under aerobic conditions, and their ghosts were subsequently solubilized without cross-linking (Fig. 2). We concluded that under the latter conditions, the intermolecular disulfide couplings producing the high-molecular-weight membrane protein polymer took place spontaneously during aerobic incubation.

Densitometric scan of the large complex of cross-linked ghosts from ATP-depleted red cells is illustrated in Figure 3 and compared to a reference sample of normal mem-

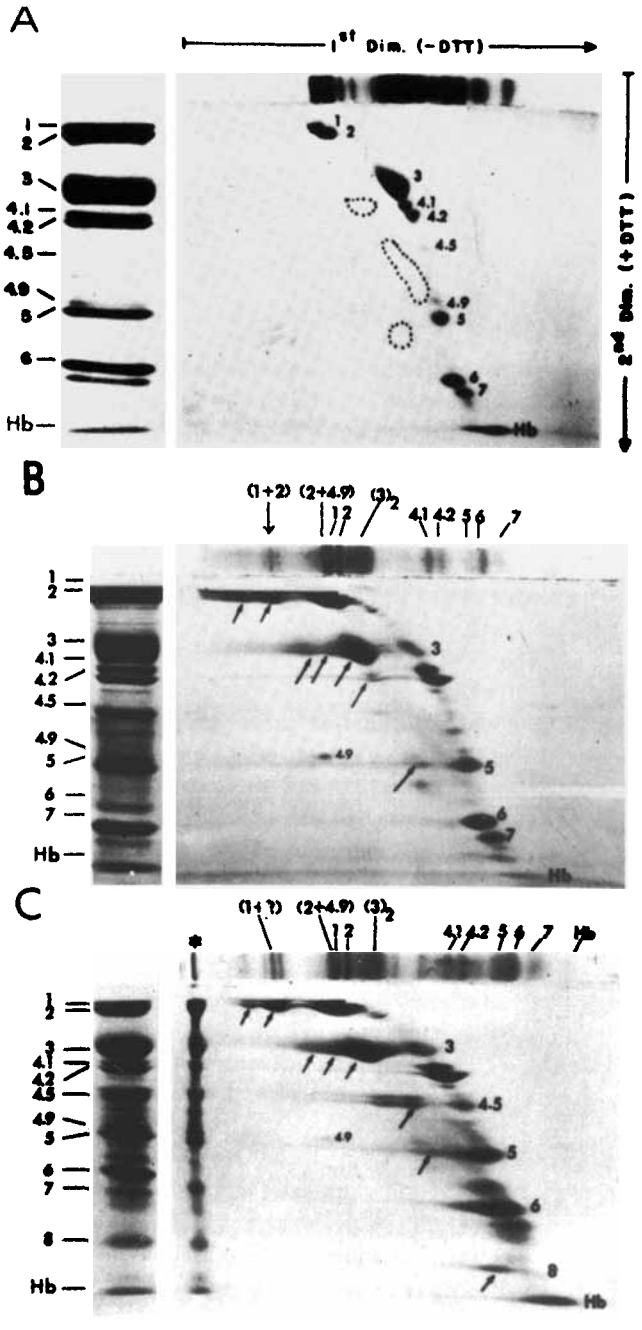
A
1st Dim. (-DTT)
2nd Dim. (+DTT)
1
2
3
4.1
4.2
4.5
4.9
5
6
7
8
Hb
B
(1+2)
(2+4.9)
(3)2
C
*

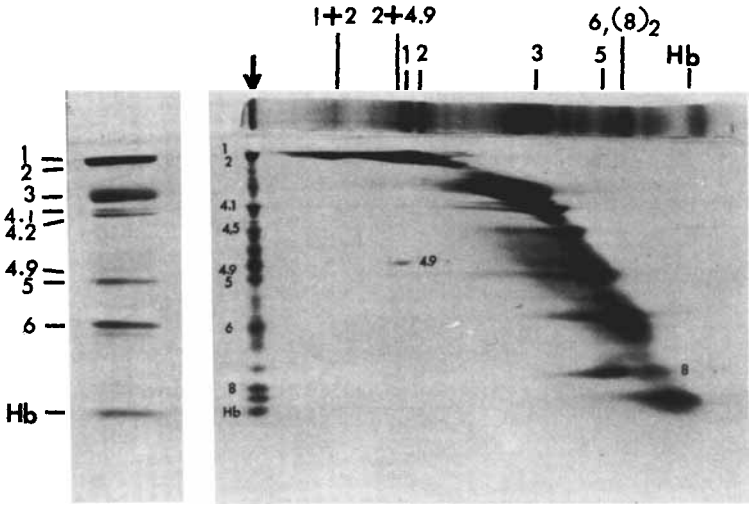

Fig. 2. Two-dimensional PAGE of membrane proteins (250 μg) from red cells depleted in ATP by incubation under air for 24 hours. These were not subjected to catalytic oxidation. Arrow indicates a spontaneously formed large molecular weight polymer (> 10^6 daltons) in the first dimension and the cleaved components in the second dimension. (Reprinted from Ref 14 with permission of publishers.)

Fig. 1. Two-dimensional PAGE of cross-linked proteins ($CuSO_4$/O-phenanthroline) in isolated membranes from fresh and ATP-depleted erythrocytes.

A) Fresh ghosts (100 μg protein) that were not subjected to cross-linking were fractionated in the first dimension by electrophoresis in SDS agarose (0.3%)-polyacrylamide (2.5%) composite gels without DTT reduction. Electrophoresis in the second dimension was performed in a slab, incorporating a DTT zone to cleave the possible disulfide bonds. The pattern of membrane sample applied directly is shown at the left for reference. The pattern obtained by electrophoresis in the first dimension is shown in a stained replicate gel placed on top of the slab. Off-diagonal elements indicated by a dotted curve probably represents glycoproteins. The indiviudal polypeptides are numbered according to Fairbanks et al [22].

B) Ghosts from fresh erythrocytes were cross-linked by catalytic oxidation with $CuSO_4$ (10 μM) + O-phenanthroline (50 μM) at 25°C for 10 min. Membrane proteins were electrophoresed in the first dimension without a prior DTT reduction. Second dimension was run as described in Figure 1A. Arrows indicate polymers of spectrin – ie, (1 + 2), $(1 + 2)_2$ – band 3 – ie, $(3)_2$, $(3)_3$, $(3)_4$ – and dimers of 4.1, 4.5, and 5.

C) Ghosts from ATP-depleted erythrocytes (37°C, under nitrogen, 24 hours) were analyzed as in Figure 1B. The asterisk at the origin represents the large molecular weight polymer (>1 X 10^6 daltons). Note also a dimer of band 8. (Reprinted from Ref 23 with permission of publishers.)

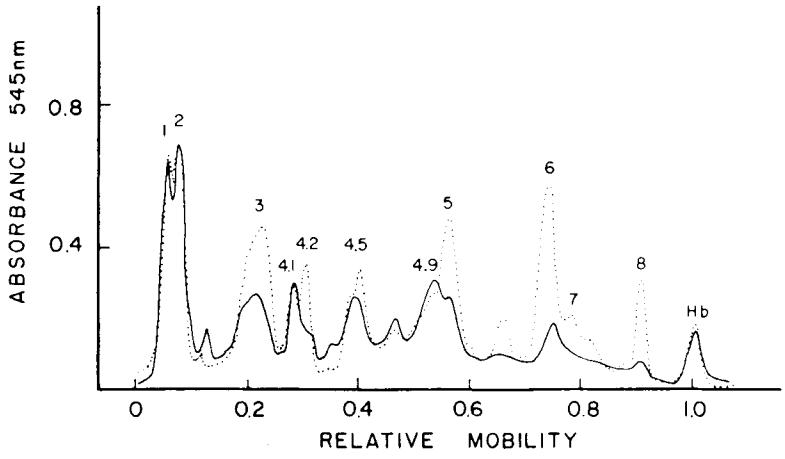

Fig. 3. Densitometric scans of Coomassie blue-stained proteins released from the $> 1 \times 10^6$ daltons polymer after DTT reduction. (This polymer is depicted in Figure 1C.) Dotted line shows a reference membrane sample separated in an identical gel system. (Reprinted from Ref 23 with permission of publishers.)

brane proteins separated in an identical gel system. It can be seen that this high-molecular-weight complex was selectively enriched in spectrin, whereas the ratio of band 3 to spectrin (0.45) was considerably less than in normal red cell membranes (1.0). In the following text, this large complex of mw $> 1 \times 10^6$ is referred to as spectrin-rich polymer.

Glutaraldehyde Cross-Linking

We investigated whether the spectrin-rich polymer of ATP-depleted red cells reflected an altered spectrin organization in the membrane in which spectrin neighbors came into closer contact. For this we employed another cross-linking agent, glutaraldehyde, which produces irreversible cross-links between the adjacent amino groups in the red cell membrane.

Glutaraldehyde cross-linking of red cells depleted of ATP under anaerobic conditions produced a polymer resembling that produced by catalytic oxidation in failing to enter the gel. In contrast, such polymers were not formed by glutaraldehyde cross-linking of ghosts from fresh cells (not shown). Reproducible demonstration of differences in membrane protein cross-linking between fresh and ATP-depleted red cells required careful maintenance of temperature, time, and concentration of the reactants. Increased temperature, cross-linking times or concentrations of these reagents produced high-molecular-weight complexes both in membranes of depleted and fresh cells, presumably due to membrane perturbation resulting from a more extensive cross-linking.

ATP Dependence on the Spectrin-Rich Polymer

Spontaneous formation of the spectrin-rich polymer is markedly dependent on red cell ATP content, as illustrated in Fig. 4. The amount of spectrin-rich polymer increases progressively as red cells undergo ATP depletion under aerobic conditions. The formation of this complex was completely inhibited by maintenance of red cell ATP level (Fig. 4B, 1st gel). In addition, aerobically ATP-depleted erythrocytes exhibited a spontaneous formation of two additional complexes of mw, 450,000 and 260,000. These represented complexes 1 + 2 and 2 + 4.9, respectively, as documented by analysis in the second dimension after DTT reduction, shown in Fig. 2.

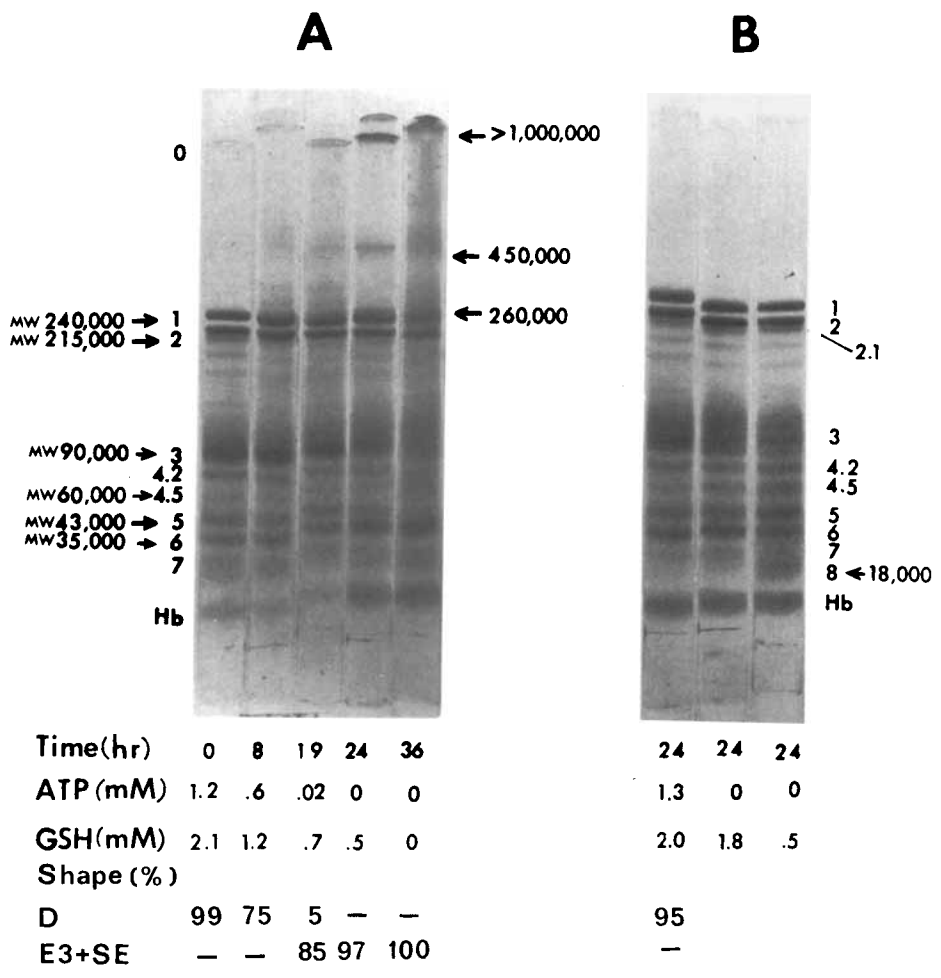

Fig. 4. Formation of large molecular weight complexes of membrane proteins during red cell ATP depletion in vitro.
A) Relationships between changes in red cell ATP, GSH, shape, and membrane protein composition during aerobic incubation of red cells at 37°C without glucose. Membrane proteins were separated by electrophoresis in SDS agarose (0.3%)-acrylamide (2.5%) composite gels without DTT reduction.
B) Inhibition of the formation of large molecular weight complexes by a maintenance of red cell ATP with adenine (0.5 mM), inosine (12.7 mM), glucose (2 gm/liter, 1st gel), anaerobic incubation (N_2, 2nd gel), or DTT (25 mM) reduction before electrophoresis (3rd gel). D, E3, and SE depict the percent of discocytes, echinocytes 3, and spheroechinocytes classified according to Ref 24. (Reprinted from Ref 14 with permission of publishers.)

The bottom part of Fig. 4 indicates a relationship of the spectrin-rich complex to cellular shape. It can be seen that appreciable amounts of the spectrin-rich polymer were noted in cell populations showing 80% conversion to echinocytes 3 or spheroechinocytes (classified according to Bessis [247]). ATP repletion was associated with a partial recovery of biconcave shape and a decrease (40–60%) in the staining intensity of the high-molecular-weight complex (not shown). The spectrin-rich polymer was absent in cross-linked ghosts from red cells in which echinocytic shape was produced by lysolecithin (0.1 mM). On the other hand, a spectrin-rich complex was noted in aerobically ATP-depleted erythrocytes

in which biconcave shape was maintained by the addition of cationic anesthetic (such as 40 mM procaine HCl) to the incubation medium (not shown). These data indicate direct relationships of the spectrin-rich polymer to cellular ATP content; on the other hand, ATP-independent shape changes appeared to be without effect on the formation of this polymer.

Since aerobic ATP depletion or ghost exposure to catalytic oxidation is associated with a marked decrease in GSH, we investigated the relative contributions of GSH and ATP in the formation of the spectrin-rich polymer and the complexes of 1 + 2 and 2 + 4.9. We have incubated G6PD-deficient red cells aerobically with adenine, inosine, and glucose and an oxidant, acetylphenylhydrazine (4 mM). These cells maintained normal ATP levels (70% of preincubation value) while they exhibited a marked GSH depletion (10% of preincubation value). The oxidative injury to these cells was manifested morphologically by the formation of five or more Heinz bodies per cell in more than 90% of these cells (not shown). As shown in Figure 5, such cells exhibited spontaneous formation of spectrin heterodimer 1 + 2 and a complex of 2 + 4.9. They further contained a high-molecular-weight protein complex at the start of the first-dimension gel (arrow of Fig. 5); however, after dissociation by DTT and subsequent separation in the second dimension, this polymer was found to consist almost exclusively of globin subunits. Thus, oxidative damage to cells containing normal ATP content resulted in an extensive disulfide coupling of globin and a formation of complexes 1 + 2 and 2 + 4.9. However, it failed to produce the large spectrin-rich polymer.

The above data suggest that the spontaneous formation of the high-molecular-weight spectrin-rich polymer of ATP-depleted red cells is a consequence of two processes. First, spectrin and other membrane proteins rearrange to close contact with each other, presumably because of protein aggregation. Second, these aggregated proteins are subsequently coupled by disulfide cross-links. These take place spontaneously when ATP depletion is performed under aerobic conditions. We have shown that i) the first process, that is, the "rearrangement" of spectrin, is prevented by a maintenance of ATP content, and ii) the

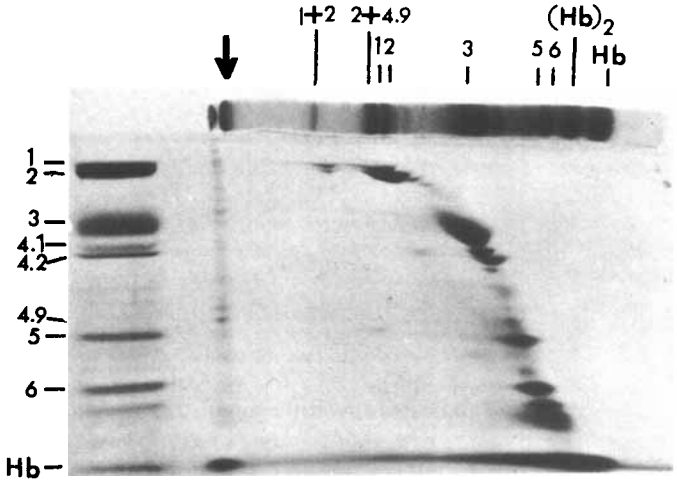

Fig. 5. Two-dimensional PAGE of membrane proteins of acetylphenylhydrazine-treated G6PD-deficient erythrocytes. Red cells were incubated under air with 4 mM acetylphenylhydrazine for 3 hours. Arrows indicate the large aggregate at the origin of the first dimension. (Reprinted from Ref 14 with permission of publishers.)

second process can be reversed by reducing agents which dissociate the above disulfide cross-links. We further explored whether the first process, ie, the spectrin "rearrangement," is reversible with ATP repletion. We have depleted red cells in ATP under anaerobic conditions (to prevent a spontaneous protein disulfide coupling) and subsequently restored ATP content with adenine and inosine. Ghosts from both ATP-depleted and -repleted cells were subsequently subjected to cross-linking with catalytic oxidation and examined for the presence of spectrin-rich polymer. Maintenance of ATP content completely suppressed the propensity of the cells to form the spectrin-rich complex after catalytic oxidation. In contrast, ATP-depleted red cells in which the ATP content was subsequently restored to 40–60% of the original level (90% of which recovered their discoidal shape) continued to form this polymer after a subsequent catalytic oxidation (not shown). This suggests that the rearrangement of spectrin to closer contacts, as reflected by the formation of this complex, is ATP-dependent. However, once this rearrangement occurs, it cannot be reversed by a subsequent ATP repletion, and it does not appear to relate directly to changes in cell shape.

Role of Calcium

Since shape and deformability alterations of red cells undergoing ATP depletion can be mimicked by introduction of calcium into red cells or ghosts [5, 8, 25, 26], we tested the role of Ca^{++} in the formation of the spectrin-rich polymer The following three approaches were used. First, exclusion of calcium from the incubation medium failed to prevent the formation of this complex during aerobic incubation without metabolizable substrates (not shown).

Second, we tested the effect of chelating agents on ghosts of ATP-depleted red cells. We have previously observed that the calcium accumulating in red cell membranes during ATP depletion was nearly completely extracted by washing ghosts with EDTA [27]. However, EDTA washing did not prevent the formation of spectrin-rich polymer after catalytic oxidation of ghosts from ATP-depleted red cells (not shown).

The third approach consisted in loading fresh red cells or their ghosts with increasing calcium concentration. When red cells were exposed to the calcium ionophore A23137 and 0.1 mM Ca^{++} (60 min, 37°C) and their ghosts were subsequently subjected to oxidative cross-linking, a high-molecular-weight complex was again found, provided that the same concentration of external calcium was maintained during ghost preparation prior to cross-linking (not shown). However, such cells also exhibited a decrease in ATP (to 40% of preincubation values), as also shown by others [28].

Exposure of washed, white ghosts to Ca^{++} followed by oxidative cross-linking failed to produce a reducible high-molecular-weight polymer unless the Ca^{++} concentration exceeded 2 mM. The introduction of 10^{-6} to 10^{-4}M Ca^{++} into ghosts during hemolysis, followed by oxidative cross-linking, produced an extensive background smearing which did not permit examination of the above high-molecular-weight protein complexes (not shown). Hemolysis in Ca^{++} at 0.5 mM followed by incubation at 37°C yielded spontaneous formation of a protein polymer at the start of the gel (Fig. 6) which differed from the spectrin-rich polymer of ATP-depleted red cells by its complete resistance to DTT cleavage. This polymer could not be reproduced when ghosts were washed prior to the exposure to calcium. However, a subsequent addition of a ghost-free hemolysate restored the spontaneous formation of this complex (not shown). In contrast to fresh red cells, ATP-depleted erythrocytes (both under O_2 or N_2) exposed to similar calcium concentrations during hemolysis failed to produce such a complex. Subsequent exposure of

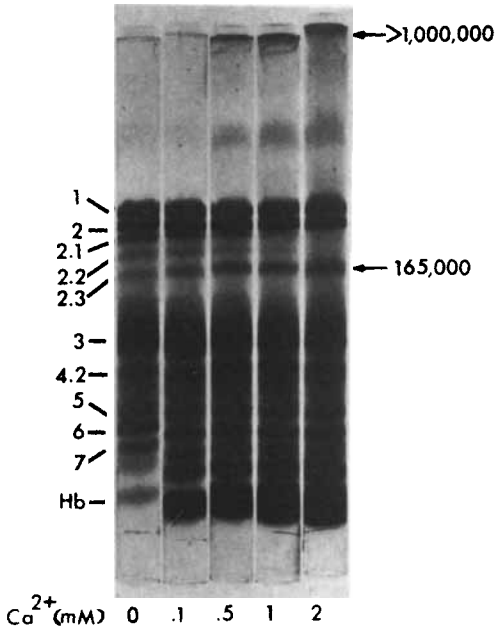

Fig. 6. Ca^{2+}-induced membrane protein polymerization. Fresh washed erythrocytes were lysed with 10 mM Tris buffer, pH 7.4, containing various Ca^{2+} concentrations and incubated at 37°C for 30 min. Ghosts were subsequently washed twice with 10 mM Tris, pH 7.4, and then subjected to PAGE in the presence of DTT. (Reprinted from Ref 23 with permission of the publishers.)

washed ghosts from ATP-depleted red cells to a ghost-free hemolysate from fresh red cells restored their propensity to form the high-molecular-weight nonreducible polymer. These data suggest i) requirement of a cytoplasmic constituent for polymer formation and ii) its dependence on intracellular ATP levels (eg, inhibition by ATP depletion). Others have shown that the formation of this polymer is related to calcium activation of cytoplasmic transglutaminase, which forms covalent cross-links among δ-glutamyl–ε-lysine residues of spectrin, band 3, and presumably other membrane and cytoplasmic proteins [29, 30]. The enzyme is dependent on ATP level [31].

Stabilization of Red Cell Shape by Membrane Protein Polymerization

Since some cross-linking agents are used as biologic fixatives, we investigated whether the above-mentioned membrane protein polymers contributed to irreversibility of spheroechinocytic shape. Table I depicts the propensity of ATP-depleted echinocytes to resume biconcave shape after a subsequent ATP repletion. The restoration of ATP levels in red cells previously depleted of ATP under aerobic conditions (producing the spectrin-rich polymer in the membrane) was associated with a considerably slower and incomplete restoration of biconcave shape when compared to anaerobically ATP-depleted red cells which did not form the complex spontaneously [14]. The exposure of the cross-linked cells to DTT reduction (which completely dissociates the polymer) markedly improved their ability to resume biconcave shape. No major differences were noted in the kinetics of restoration of ATP levels under both conditions (Table I). These data suggest that the delayed and incomplete reversal of aerobically ATP-depleted echinocytes to discocytes

TABLE I. Restoration of Biconcave Shape and ATP and GSH Levels of ATP-Depleted Red Cells During Subsequent Incubation (37°C) With Glucose, Adenine, and Inosine*

	Time (hours)			
	0	1	2	4
Discocytes (%)				
N_2	0	92	98	98
O_2	0	31	48	68
O_2 & DTT	0	86	88	89
ATP (%)				
N_2	10	32	38	37
O_2	10	30	32	33
Air & DTT	10	31	30	32
GSH (%)				
N_2	90	80	90	100
O_2	0	35	65	75

*Red cells were depleted in ATP by 18 hours (37°C) of incubation without glucose under 100% nitrogen or oxygen. DTT was added at a final concentration of 4 mM. Mean values of three experiments. ATP and GSH are expressed as % of preincubation levels.

TABLE II. Dependence of the Formation of the Nonreducible Membrane Protein Polymer and the Percentage of Irreversible Spheroechinocytes on Ca^{2+} Concentration

External Ca^{2+} concentration (mM)[a]	0.1	0.5	1.0	2.0	2.0 + histamine
Nonreducible[b] polymer (%)	0	7	25	100	8
Irreversible spheroechinocytes (%)[c]	7	12	36	100	11

[a]Fresh red cells were exposed to A23187 and Ca^{2+} (1 hour, 37°C). Histamine concentration (last column) was 40 mM.
[b]The polymer is expressed as percent of the amounts produced by 2 mM Ca^{2+}, as measured planimetrically after densitometric scanning of Coomassie blue-stained gels.
[c]Counted after 16 hours of incubation with glucose, adenine, and inosine. ATP was repleted to 80–120% of preincubation values and > 95% of ^{45}Ca was extruded from the cells after incubation. Mean values of four experiments.

during ATP repletion was related to oxidative cross-linking of membrane proteins which stabilized the altered spectrin arrangement in such cells.

The nonreducible polymer produced by 0.5 mM Ca^{++} + A23187 had a similar stabilizing effect on cell shape. Table II illustrates that a progressively increased formation of this complex, produced by exposure of cells to increasing external concentrations of Ca^{++} (in the presence of A23187) coincided with increased percentage of cells which retained spheroechinocytic shape after a subsequent ATP repletion and extrusion of calcium from the cells. Transglutaminase inhibition by histamine prevented the formation of the nonreducible polymer and nearly completely restored the propensity of such cells to transform into biconcave and stomatocytic shapes (Fig. 7).

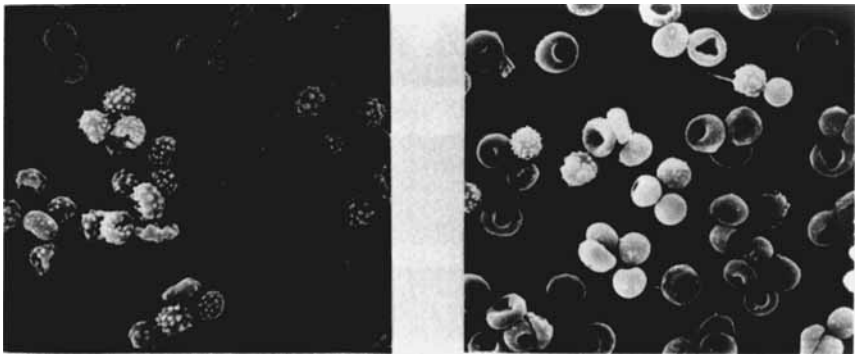

Fig. 7. 1. SEM of red cells treated with 2 mM Ca^{2+} and A23187 for 1 hour, followed by 17 hours of incubation with glucose, adenine, and inosine (left). 2. The SEM on the right depicts the same conditions, except that 40 mM histamine was present at the time of exposure of cells to Ca^{2+}.

Irreversibly Sickled Cells

The calcium content of ISC-enriched (54 ± 8%) HbSS red cells is higher than that of non-ISC HbSS cells (ISCs: 66 ± 12 μmoles/liter cells; unseparated HbSS red cells: 50 ± 21 μmoles/liter cells). It is almost four times higher than that of normal erythrocytes (18 ± 6 μmoles/liter of cells [9]. Furthermore, ISCs exhibit a decrease in ATP content [11, 12]. We have examined ISC membrane protein composition in order to evaluate a possible role of the membrane protein polymerization in irreversibly sickled shape.

ISCs were separated from blood of individuals with the homozygous form of sickle cell anemia (HbSS) using a five-step discontinuous stractan gradient. HbSS red cells were separated thereby into five fractions (Fig. 8). Fraction 1 (top) contained no ISCs; fractions 3, 4, and 5 all contained > 80% ISCs. Fractions 1–5 also exhibited progressively increasing mean corpuscular hemoglobin concentrations (MCHC) from 34 to 41% and decreasing mean volumes (MCV) from 96 to 61. ISCs from the two densest fractions were subsequently washed and subjected to analysis of membrane protein composition before and after cross-linking with catalytic oxidation or glutaraldehyde.

Figure 9A illustrates protein composition of ISC-free HbSS red cell ghosts (fraction 1), HbSS cells containing 90% ISCs (fraction 4 + 5), and ghosts, from aerobically ATP-depleted red cells. It is apparent that both ISC-free and ISC-rich HbSS red cells failed to exhibit large complexes of proteins in untreated membranes. However, both ISCs and to a lesser extent non-ISC HbSS cells shared with ATP-depleted red cells an increased retention of band 4.5 (membrane-attached catalase [33, 34]) and globin. Likewise, ISC membrane protein cross-linking with both catalytic oxidation (Fig. 9B) and glutaraldehyde (not shown) failed to produce high-molecular-weight protein complexes in these membranes under conditions that readily induce cross-linking in membranes from ATP-depleted cells. Thus, the ISC lesion does not appear to result from a stabilization of ISC shape by membrane protein cross-linking; presumably the degree of ATP depletion and calcium accumulation in ISCs is not sufficiently high to produce these changes.

ISC-Spheroechinocyte Transformation

Figure 10 depicts scanning electron micrographs of ISCs from fractions 3 and 5. It is apparent that ISCs exhibited a considerable morphologic heterogeneity: ISCs of relatively low densities (fraction 3) had an elongated shape with a central concavity, while 5–10%

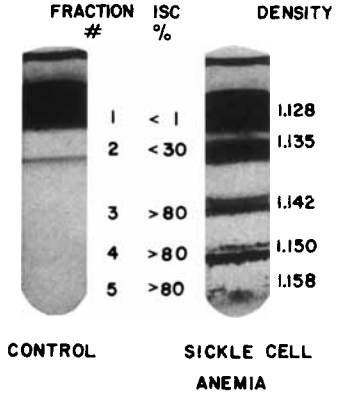

Fig. 8. ISC separation on a discontinuous stractan gradient. (Reprinted from Ref 32 with permission of publishers.)

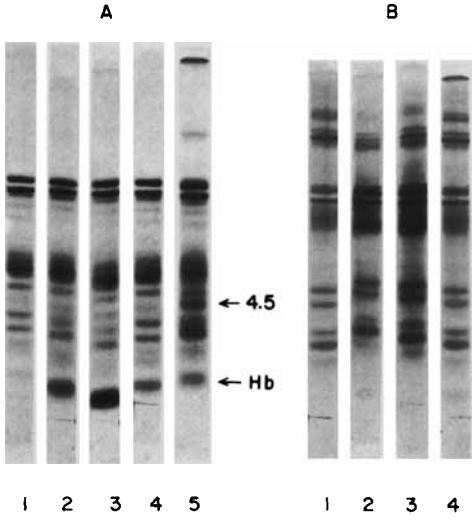

Fig. 9. PAGE of ISC ghost proteins before (A) and after (B) cross-linking by catalytic oxidation, as described in Figure 1. All samples were prepared in the absence of DTT. Otherwise, the gel system was the same as that described in Figure 3. 1) Fresh normal red cells; 2) Top HbSS fraction 1 containing no ISCs; 3) Bottom ISC-rich fractions 4 + 5 (combined); 4) ATP-depleted red cells (22 hours, 37°C) under anaerobic conditions; 5) ATP-depleted red cells under aerobic conditions. (Reprinted from Ref 23 with permission of publishers.)

of the densest cells (fraction 5) had an elliptical shape and an extensive surface speculation. These shape changes were not artifacts of stractan separation, as pooling of all the cells followed by differencial counting yielded a percentage of echinocytic ISCs (1%) similar to the fresh, unseparated HbSS blood. These data suggest that ISCs undergo a discocyte-to-echinocyte transformation in vivo, presumably as a result of progressively increasing calcium accumulation and ATP depletion.

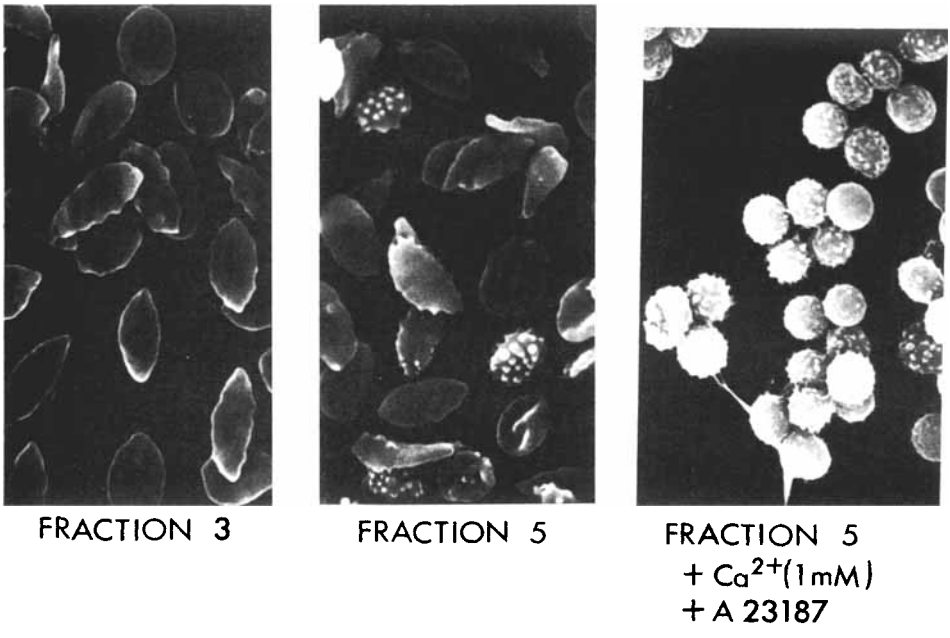

Fig. 10. SEM of ISCs from fraction 3, fraction 5, and combined fractions 4 + 5 exposed to Ca^{2+} (1 mM) and calcium ionophore A23187 (10 μM) for 60 min at 37°C. (Adapted from Refs 23 and 32 with permission of publishers.)

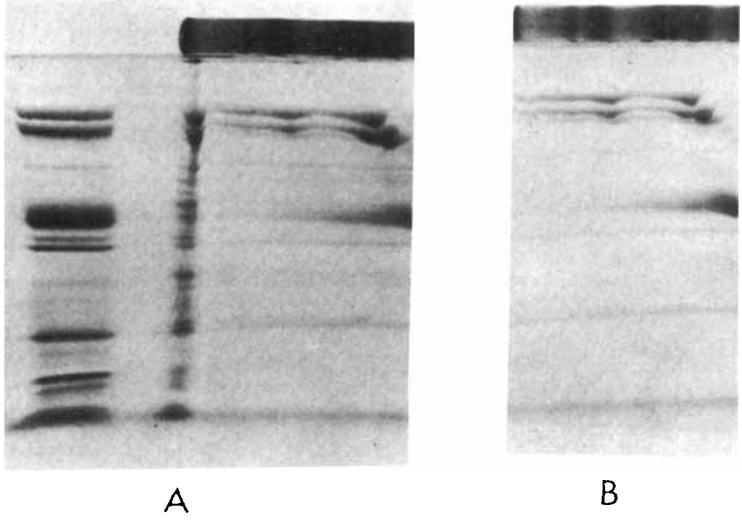

Fig. 11. Accelerated formation of the spectrin-rich complex during incubation (6 hours, 37°C) of ISCs without glucose. A) ISC-rich fractions 4 + 5 (combined); B) HbSS cells from fraction 1, containing no ISCs. Cross-linking of ghosts from incubated ISCs and PAGE was done as described in Figure 1. (Reprinted from Ref 32 with permission of publishers.)

The above hypothesis is supported by the data shown in Fig. 10, which illustrates that ISCs (fraction 5, 90% ISCs) can be efficiently (90%) converted into spheroechinocytes after exposure to 2 mM Ca^{++} + A23187. Furthermore, ISCs exhibited an increased propensity to form the spectrin-rich reducible polymer during aerobic incubation without glucose. Figure 11 illustrates that after 6 h of incubation, the top, ISC-free HbSS red cells did not form any spectrin-rich polymer, while the dense ISC-rich fraction 4 + 5 produced considerable amounts of this complex. More than 80% of these incubated ISCs were converted to type 3 echinocytes or spheroechinocytes (not shown). The increased propensity of ISCs to form the spectrin-rich reducible complex and transform into echinocytic shapes during a subsequent incubation without glucose is presumably related to their decreased ATP and increased calcium content in vivo.

DISCUSSION

ATP-Calcium Dependence of Membrane Protein Organization

Our cross-linking studies revealed major differences between the nearest membrane protein neighbors of fresh and ATP-depleted red cell membranes. Oxidation of the intermolecular SH groups of fresh red cell ghosts resulted in formation of dimers and tetramers of spectrin, dimers of band 3 and actin, and a 2 + 4.9 complex. In contrast, disulfide coupling of ATP-depleted erythrocyte ghosts produced an additional protein complex of $mw > 1 \times 10^6$ (Table III).

This polymer was produced by three different types of cross-linking: a) $CuSO_4$, O-phenanthroline-catalyzed intermolecular disulfide coupling, b) spontaneous disulfide couplings in intact red cells during their aerobic ATP depletion, and c) glutaraldehyde cross-linking. The reducible polymer of ATP-depleted red cells was selectively enriched in spectrin, while the relative amounts of actin and band 3, the major transmembrane polypeptide, were lower than in normal red cell membranes. We conclude that red cell ATP depletion alters spectrin organization within the membrane to produce more intimate contacts, which in turn allow an easier cross-linking of the individual spectrin subunits into the large polymer. It is not likely that the increased propensity of spectrin to cross-linking relates to 1) a conformational change exposing a previously masked SH group, or 2) a dissociation from the membrane binding site that increases its lateral mobility and hence increases the chance of collisions. The first possibility is unlikely because other agents, such as glutaraldehyde, which cross-links protein amino groups, produced a similar polymer. Likewise, we exclude the second possibility, as the cross-linking could also be produced at temperatures close to 0°C, when membrane proteins exhibit only a limited lateral mobility.

The dependence of the formation of spectrin-rich polymer on red cell ATP depletion is suggested by an absence of this polymer in cells in which ATP has been maintained during incubation. These ATP-maintained cells failed to exhibit this polymer after cross-linking with both catalytic oxidation and glutaraldehyde. In contrast, this polymer was produced by the above-mentioned cross-linkings in cells which were first depleted in ATP and subsequently ATP-repleted by incubation with adenine-inosine, which suggests an irreversibility of the ATP-dependent reorganization of spectrin to closer contacts. It should be pointed out that the partial disappearance of this complex during ATP repletion of cells previously depleted in ATP under aerobic conditions should not be interpreted as indicating the reversibility of this process. Under the latter circumstances, cells apparently generate a reducing power which cleaves the disulfide cross-linkages but spectrin remains rearranged into closer contacts.

TABLE III. Oxidative Membrane Protein Cross-Linkings of Fresh and ATP-Depleted Red Cells

	Fresh	ATP-depleted
$(1 + 2)_2$	+	+
(2 + 4.9)	+	+
$(3)_2$	+	+
$(5)_2$	+	+
Spectrin-rich (10^3K) complex	–	+

Polymer formation is apparently not controlled by intracellular Ca^{++}, but our data on this point are not conclusive. First, the formation of the spectrin-rich polymer during aerobic ATP depletion was not influenced by exclusion of calcium from the incubation medium. However, normal red cells contain 3.5 μM of exchangeable calcium per liter of cells (presumably as a calcium ATP complex [27]), which after depletion of intracellular ATP may interact with the membrane, thereby producing the spectrin-rich polymer even in the absence of a net calcium accumulation. Second, Ca^{++} treatment of washed, white ghosts from fresh red cells, followed by oxidative cross-linking, failed to produce the polymer unless the Ca^{++} concentrations exceeded 2 mM. In contrast, treatment of fresh red cells with 0.1 mM Ca^{++} + A23187 virtually duplicated the effects of ATP depletion. However, these cells also exhibited a marked decrease in intracellular ATP. Third, the exposure of ghosts from anaerobically ATP-depleted cells to EDTA, which extracts calcium accumulating in membranes of ATP-depleted red cells [27], failed to prevent the formation of this polymer after subsequent ghost cross-linking with catalytic oxidation. The latter data suggest, but do not prove, that ATP depletion alone rather than a concomitant calcium-membrane interaction is responsible for changes in spectrin organization of ATP-depleted erythrocytes.

In contrast to the formation of a reducible spectrin-rich polymer in ATP-depleted erythrocytes, red cells exposed to 0.5 mM Ca^{++} + A23187 spontaneously produced a high-molecular-weight polymer which resisted cleavage by DTT. This complex was recently shown to result from covalent cross-links between δ-glutamyl–ϵ-lysine residues of the nearest spectrin, band 3, and other membrane protein neighbors catalyzed by a Ca^{++}-activated cytoplasmic transglutaminase [29, 30]. This polymer could not be reproduced in ATP-depleted red cells, presumably because the enzyme is inhibited by ATP depletion [31].

Role of Spectrin-Rich Polymer in Discocyte-Echinocyte Equilibrium

Several laboratories [35–38] provided indirect support for the hypothesis that the stomatocyte-discocyte-echinocyte equilibrium depends on the relationships between the surface areas of the inner and outer halves of the membrane lipid bilayer. We speculate that the echinocyte transformation of ATP-depleted red cells is related to a reorganization of spectrin to establish closer contacts. Assuming that spectrin and actin form a two-dimensional network [4], this rearrangement could produce a decrease in surface area both of the spectrin-actin network and the closely associated inner half of the membrane lipid bilayer. The resulting bilayer asymmetry would then be reflected in an echinocytic shape change. However, this model cannot account for the observation that during ATP repletion cells restore their biconcave shape despite the fact that spectrin remains reorganized into closer contacts.

Although no direct comparisons between the formation of the reducible spectrin-rich polymer and changes in membrane deformability are to be found in the literature, it is likely that altered spectrin interactions in ATP-depleted red cells may result in changes of membrane deformability. This possibility is suggested by recent observations of decreased membrane deformability of cells exposed to cross-linking agents such as glutaraldehyde [39] and kinetic similarities in the formation of spectrin-rich polymer and changes in red cell deformability [5, 14].

Irreversibly Sickled Cells

ISCs which maintain their characteristic elongated shape even after prolonged oxygenation are rigid, dehydrated cells with a markedly shortened survival in the circulation (for references see Palek [13]). ISC shape deformation has also been found in ghosts and in spectrin-actin residues prepared by extraction of lipids and integral membrane proteins from red cell membranes [40].

Since both the reducible spectrin-rich polymer of aerobically ATP-depleted red cells and the nonreducible polymer of calcium-enriched fresh erythrocytes contributed to a stabilization of red cells in the spheroechinocytic configuration, and since ISCs exhibit increased calcium and decreased ATP content, we evaluated the role of membrane protein polymerization in the stabilization of ISC shape.

Although HbSS red cell separation on the discontinuous stractan gradient allowed us to isolate HbSS red cell populations containing > 90% USCs (Fig. 8), we were unable to find either of the two polymers in freshly isolated ISCs, including the densest ISC-rich fraction 5 (Fig. 9). Likewise, no high-molecular-weight polymer was seen after a subsequent exposure of ISC ghosts to cross-linking by catalytic oxidation or glutaraldehyde. Thus, it is unlikely that spectrin rearrangement and polymerization contributed to a permanent shape fixation of these cells, presumably because the calcium gain and ATP depletion in ISCs did not reach the levels required for spectrin rearrangement and polymerization.

The shape heterogeneity of ISCs separated on a discontinuous stractan gradient suggested that ISCs undergo an ISC discocyte-to-echinocyte transformation in vivo which may be related to a progressive calcium accumulation and ATP depletion in these cells. This possibility is supported by the following findings. First, ISC exposure to Ca^{++} + A23187 resulted in their transformation to spheroechinocytes. Second, during incubation without glucose, ISCs formed a spectrin-rich polymer considerably earlier than the non-ISC HbSS red cells; at the same time, the incubated ISCs assumed an echinocytic shape. Third, when ISCs were formed in vitro during incubation of deoxygenated HbSS red cells under conditions leading to progressive ATP depletion and calcium accumulation, the resulting ISC-shaped cells exhibited an extensive surface spiculation [27]. In contrast, when deoxygenated HbSS red cells were incubated in the absence of the external calcium and under conditions maintaining intracellular ATP levels, the resulting in vitro ISCs lacked a surface spiculation and occasionally exhibited a central concavity.

On the basis of these observations, we conclude that the permanent stabilization of ISC shape does not require ATP depletion and calcium accumulation. In contrast, the additional physical alterations of ISCs, namely, their dehydration [41], decreased deformability, and ultimately echinocyte transformation, may be related to a progressive calcium accumulation and ATP depletion of these cells. The preferential calcium accumulation in ISCs may be related to their high concentration of hemoglobin S relative to hemoglobin F [19] and a known dependence of calcium influx on the concentration of hemoglobin S in the cells [9]. Thus, the progressive calcium accumulation and ATP depletion in ISCs may result in their progressive dehydration, decrease deformability, and ultimately a trans-

formation into spheroechinocytic ISCs. Presumably, the latter ISCs represent an end-stage lesion, resulting in a removal of these cells from circulation.

ACKNOWLEDGMENTS

This study was supported by National Institutes of Health grant HL15157. We appreciate the skilled technical help of Maureen Monroe, Brian Timura, and Robert Lundin.

REFERENCES

1. Evans EA, Hochmuth RM: J Membrane Biol 30:351, 1977.
2. Evans EA, LaCelle PL: Blood 45:29, 1975.
3. LaCelle PL, Kirkpatrick FH: Erythrocyte Structure and Function (Proc 3rd Int Conf Red Cell Metabolism and Function) 535, 1974.
4. Steck TL: J Cell Biol 62:1, 1974.
5. Weed RI, LaCelle PL, Merrill EW: J Clin Invest 48:795, 1969.
6. Lux SE, John KM: In Revel JP, Henning U, Fox CF (eds): "Cell Shape and Surface Architecture." New York: Alan R Liss, 1977.
7. Lutz HU, Liu SC, Palek J: J Cell Biol 73:548, 1977.
8. Palek J, Stewart G, Lionetti FJ, Blood 44:583, 1974.
9. Palek J: J Lab Clin Med 89:1365, 1977.
10. Eaton JW, Skelton TD, Swofford HS, et al: Nature 246:105, 1973.
11. Weed RI, Bessis M: Clin Res 23:442A, 1975.
12. Glader BE, Lux SE, Muller A, et al: Clin Res 24:309A, 1976.
13. Palek J: Br J Haematol 35:1, 1977.
14. Palek J, Liu SC, Snyder LM: Blood 51:385, 1978.
15. Steck TL: J Mol Biol 66:295, 1974.
16. Wang K, Richards FM: J Biol Chem 249:8005, 1974.
17. Liu SC, Fairbanks G, Palek J: Biochemistry 16:4066, 1977.
18. Corash LM, Piomelli S, Chen AC, et al: J Lab Clin Med 84:147, 1974.
19. Bertles JF, Milner P: J Clin Invest 47:1731, 1968.
20. Palek J, Liu A, Liu D, et al: Blood 50:1955, 1977.
21. Beutler E: "Red cell metabolism – A Manual of Biochemical Methods," ed 2. New York: Grune & Stratton, 1975.
22. Fairbanks G, Steck TL, Wallach DFH: Biochemistry 10:2606, 1971.
23. Palek J, Liu SC, Liu A: In Kruckenberg WC, Eaton JW, Brewer GJ (eds): "Erythrocyte Membranes: Recent Clinical and Experimental Advances." New York: Alan R Liss, 1978.
24. Bessis M: Nouv Rev Fr Hematol 12:1, 1972.
25. Kirkpatrick FH, Hillman DG, LaCelle PL: Experientia 31:653, 1975.
26. White JG: Am J Pathol 77:507, 1974.
27. Palek J, Church A, Fairbanks G: In Leaf A, Hoffman JF, Bolis L (eds): "Membranes and Diseases." New York: Raven Press, 1976.
28. Taylor D, Baker R, Hochstein P: Biochem Biophys Res Commun 76:205, 1977.
29. Lorand L, Weissman LB, Epel DL, et al: Proc Natl Acad Sci USA 73:4479, 1976.
30. Anderson DR, Davis JL, Carraway KL: J Biol Chem 252:6617, 1977.
31. Brenner SC, Wold F: Biochim Biophys Acta 522:74, 1978.
32. Palek J, Liu SC, Liu PA: In Caughey WS (ed): "Clinical and Biochemical Aspects of Hemoglobin Abnormalities." New York: Academic Press, 1978.
33. Allen DW, Cadman S, McCann SR, et al: Blood 49:113, 1977.
34. Snyder LM, Liu SC, Palek J, et al: Biochim Biophys Acta 470:290, 1977.
35. Sheetz MP, Singer SJ: Proc Natl Acad Sci USA 71:4457, 1974.
36. Sheetz MP, Painter RG, Singer SJ: J Cell Biol 70:193, 1976.
37. Palek J, Njoku G, Liu A, et al: Blood 50:155, 1977.
38. Evans EA: Biophys J 14:923, 1974.
39. Heusinkveld RS, Goldstein DA, Weed RI, et al: Blood Cells 3:175, 1977.
40. Lux SE, John KM, Karnovsky MJ: J Clin Invest 58:955, 1976.
41. Glader BF, Miller A: Pediatr Res 9:321, 1975.